energies

MDPI

Article

A Data-Driven Predictive Control Method for Modeling Doubly-Fed Variable-Speed Pumped Storage Units

Peiyu Zhao [1], Haipeng Nan [1,*], Qingsen Cai [2], Chunyang Gao [1] and Luochang Wu [1]

[1] School of Water Resources and Hydropower, Xi'an University of Technology, Xi'an 710065, China; peiyzhao@163.com (P.Z.); gcy_xaut@163.com (C.G.); wlc_xatu@163.com (L.W.)
[2] Northwest Engineering Corporation Limited, Power China, Xi'an 710065, China; caiqings@nwh.cn
* Correspondence: hxnhp@163.com

Abstract: In this study, a data-driven model predictive control (MPC) method is proposed for the optimal control of a doubly-fed variable-speed pumped storage unit. This method combines modern control theory with the dynamic characteristics of the pumped storage unit to establish an accurate dynamic model based on actual operating data. In each control cycle, the MPC uses the system model to predict future system behavior and determines the optimal control input sequence by solving the constrained optimization problem, thereby effectively dealing with the nonlinearity, time-varying characteristics, and multivariable coupling problems of the system. When compared with a traditional PID control, this method significantly improves control accuracy, response speed, and system stability. The simulation results show that the proposed MPC method exhibits better steady-state error, overshoot, adjustment time, and control energy under various operating conditions, demonstrating its advantages in complex multivariable systems. This study provides an innovative solution for the efficient control of doubly-fed variable-speed pumped storage units and lays a solid foundation for the efficient utilization of new energy sources.

Keywords: integrated energy system; modeling method; optimized control; data-driven; DFIG; MPC

Citation: Zhao, P.; Nan, H.; Cai, Q.; Gao, C.; Wu, L. A Data-Driven Predictive Control Method for Modeling Doubly-Fed Variable-Speed Pumped Storage Units. *Energies* **2024**, *17*, 4912. https://doi.org/10.3390/en17194912

Academic Editor: Nikolaos Koukouzas

Received: 13 August 2024
Revised: 15 September 2024
Accepted: 26 September 2024
Published: 30 September 2024

Copyright: © 2024 by the authors. Licensee MDPI, Basel, Switzerland. This article is an open access article distributed under the terms and conditions of the Creative Commons Attribution (CC BY) license (https://creativecommons.org/licenses/by/4.0/).

1. Introduction

Renewable energy sources are generating electricity on an ever-increasing scale, reaching 83% of newly installed power capacity worldwide in 2023 [1]. However, such a scale of intermittent energy access to the grid leads to increasingly significant grid uncertainty. The solution to this problem is to build energy storage power plants compatible with new energy sources [2]. Among the energy storage power plants, pumped storage power plants have the characteristics of a stable operation, long life, low unit cost, and environmentally friendliness. For those reasons, they have been widely used to consume new energy, adjust the peak frequency and phase, and improve the stability of the power grid [3,4]. The variable-speed technology means pumped storage units are not limited to rated speed operation, thus making the regulation more flexible, fast, efficient, and reliable. Accordingly, developing this technology has become a new direction and R&D hotspot in pumped storage worldwide [5,6]. Since a variable-speed pumped storage unit requires the coordinated operation of multiple subsystems, such as a hydraulic system and electrical system, its control system faces challenges that require it to operate with an entirely different control strategy from that of the conventional pumped storage unit [7]. Doubly-fed variable-speed pumped storage units usually include two sets of control subsystems: one is the pump-turbine control system, and the other is the doubly-fed motor control system; and the two sets of control systems usually adopt a PID control, which is easy to realize due to its simple control law. However, the operation of a variable-speed pumped storage unit has solid nonlinear characteristics, and when the operating

conditions of the unit change frequently with the grid demand, it is difficult to determine a set of control parameters that can be adapted to all operating conditions. In addition, the real-time control rate of a PID control is only related to the current and past states, and cannot predict future operating conditions. Some control strategies to improve PID focus on the optimization of controller parameters to improve the control efficiency, such as a PID control with the introduction of the elite memory mechanism particle swarm algorithm (PSO) [8]; a PID control based on Hopf bifurcation theory for stability partitioning [9]; a PID control with the introduction of the sensitivity margin index [10]; an adaptive fast fuzzy fractional-order PID (AFFFOPID) control strategy [11]; and so on.

The working principle of model predictive control (MPC) is based on the prediction and real-time optimization of the system model. In each control cycle, the MPC uses the system model to predict the system behavior in the future, and it minimizes the tracking error and the cost of the control input by setting the objective function. Subsequently, the MPC determines the control input sequence, which optimizes the objective function by solving a constrained optimization problem. Although the MPC calculates an input sequence, only the first control input is implemented in actual applications. As the system state is updated, the MPC repeats this process in each cycle, and it adjusts the control strategy through a real-time feedback mechanism, thereby effectively dealing with nonlinearity, time-varying characteristics, and multivariable coupling and realizing dynamic optimization control of the system. The PID control strategy has achieved specific effects in the control system of variable-speed pumped storage units, but there are still some shortcomings, such as failing to adapt well to the characteristics of the actual system in the processing of nonlinear dynamics, failing to satisfy the complex constraints such as power, speed, load, and other constraints in the control of the variable-speed pumped storage units; most importantly, it cannot flexibly adjust the control parameters [7,12]. As an advanced control method, the MPC has apparent advantages in dealing with complex systems, considering future prediction, flexibility and adaptability, constraints, regulation capability, and scalability. Some studies have applied MPC to variable-speed pumped storage units and achieved better results. For example, from the hydraulic perspective, one study in the literature proposed a nonlinear model predictive control strategy for controlling the pump-turbine, which improves the stability of the hydraulic system [13]. In contrast, another study in the literature proposed an enumeration-based MPC strategy that increases the hydraulic unit's operational flexibility [14]. Some other research has been conducted from an electrical point of view, and one entry in the literature proposes an MPC-based controller for direct power control of doubly-fed motors, which results in a faster and more accurate unit power output [15].

Elsewhere, one study proposes a robust continuous-time model predictive direct power control method to ensure the smooth operation of the DFIG [16]. Another considers the high-voltage ride-through (HVRT) period of the unit's bipolar blocking problem, where an MPC method based on P-Q coordination is proposed to bring the parameters to the target values under the constraints [17]. These studies entirely use the advantages of an MPC in multi-parameter tuning and effectively solve the drawback that PID control can only deal with univariate or decoupled multivariate systems. It is challenging to realize the coordinated control of complex systems. Although the MPC has many advantages, the quality and accuracy of the model determine its performance and effectiveness. Most of the existing research on variable-speed pumped storage units use mathematical models of the system, which are simplified but still present complex nonlinearities; for instance, the full characteristic curve/surface model of the main equipment pump-turbine with prominent "S" characteristics and the static and dynamic models of doubly-fed motors are both sets of higher-order differential equations [18]. In addition, there are significant errors between the model and the actual equipment due to the differences in manufacturers, capacities, and models. These factors lead to the difficulty and poor accuracy of modeling. It is worth noting that a large number of data are generated during the design, testing, and operation of variable-speed pumped storage units, which can represent the most

realistic state and underlying relationships of the equipment, can help reveal hidden patterns in complex systems, and can be used to improve the model's capacity to adapt to changing conditions [19]. Several studies have looked at data-driven approaches to MPC, to improve the control performance further. For example, one investigation used data to model a wind turbine and mitigated vortex interactions using the recently learned model predictive control (LMPC) algorithm [20]. Another study [21] transitioned from model-based to data-driven optimal control strategies in the field of motor drives, providing design guidelines for practitioners, and then worked to improve the efficiency of data utilization for an MPC, demonstrating its effectiveness in the motor current control case [22]. In the present study, we used a data-driven approach to model predictive control in the area of variable-speed pumped storage unit control, to improve the control performance of the unit. There is little related research in this area, but the few entries include some innovative research works, such as a data-driven pumped storage unit model predictive control method based on machine learning algorithms, which uses data to build a partitioned simplified model of the pump-turbine and improves the responsiveness of the unit control [23]. Moreover, another study put forward an in-line sequential limit learning machine algorithm of the model predictive control of the pumped storage unit, which can learn the coupled-system dynamic behavior and shows superiority in voltage and load adjustment and frequency oscillation suppression [24].

In this paper, a data-driven model predictive control (MPC) method is proposed to solve the problems of strong nonlinear characteristics, complex constraints, and a cumbersome parameter optimization process of a traditional PID controller in the control of variable-speed pumped storage units. An MPC can predict the future behavior of the system in real time by using actual operating data to establish an accurate dynamic model, and it can dynamically adjust the control input through an optimization algorithm in each control cycle, thus replacing the traditional PID controller's parameter adjustment method, which relies on fixed parameters. In contrast, an MPC not only simplifies the parameter adjustment process, but also more effectively adapts to the nonlinear and multivariable coupling characteristics of the system, while being able to naturally handle operational constraints. This method achieves a higher control accuracy and response speed through dynamic optimization, greatly improves the robustness of the system, and provides a more efficient and reliable variable-speed pumped storage unit control solution.

From the control effect point of view, although the MPC method proposed in this paper does not show a significant performance improvement in the control effect when compared with the PID control method we developed before. This is mainly because the variable-speed pumped storage unit is limited in its performance during actual operation, leaving limited room for improvement in the control performance. We wish to highlight that although the developed PID control method performs excellently, its parameter adjustment process is complicated, especially when the working condition is changed; the optimization program often requires a long time to calculate and the selection of the initial value of the optimization is extremely dependent on experience and skills. In contrast, the MPC method proposed in this paper successfully avoids the complexity of the traditional PID controller parameter adjustment process by dynamically adjusting the control input through real-time optimization, and it greatly simplifies the application and debugging of the controller. Therefore, we believe that this innovation provides a more efficient and practical solution for the control of variable-speed pumped storage units.

2. Integrated Modeling of Variable-Speed Pumped Storage Units

This section establishes a set of integrated models for variable-speed pumped storage units, and a brief schematic block diagram shown in Figure 1, which demonstrates the unit's operation under grid-connected conditions for power generation. The model integrates a water–machine–electricity system, and its structure is based on the whole, characteristic model of the pump-turbine, the state-space model of the double-fed motor, and the approximate elastic water hammer model of the water diversion system, which is

established by the software MATLAB/Simulink (2023b). The various components of the model are clearly described and can be flexibly combined, which is convenient for its realization, and also its further development and application.

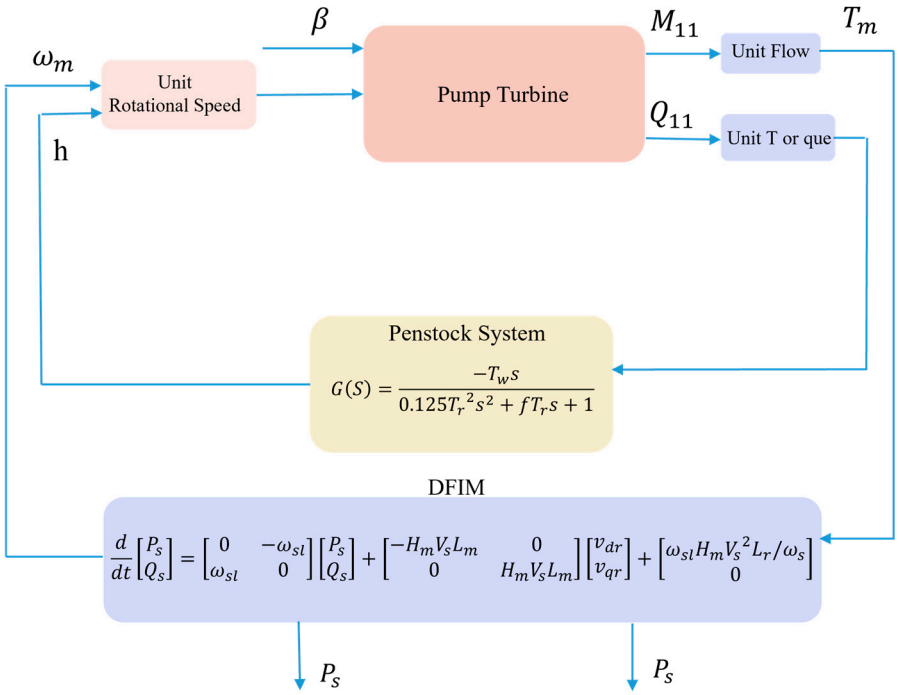

Figure 1. Schematic diagram of the integrated model of variable speed pumped storage unit.

2.1. Data-Driven Water Pump-Turbine Modeling

When modeling the pump-turbine, the full characteristic curve is used as the pump-turbine model, which is driven by experimental and actual operation data. Among these, the operation data originate from the Fujian Xianyou Pumped Storage Power Station, and the test data were sourced from the semi-physical, double-fed, variable-head and variable-speed pumped storage generator unit experimental platform based on RTDS of Xi'an University of Technology. By changing the guide vane opening and flow recording data, and using the improved Suter transformation method proposed in the literature [25], the full characteristic curve model can be obtained. This model can reflect the performance characteristics of the water pump and turbine, such as the flow rate, head, and efficiency, which is of great significance for the hydroelectric power system's design, operation, and maintenance. The whole characteristic curve reflects the relationship between unit torque, unit flow rate, unit rotational speed, and guide vane opening. The whole characteristic curve established in this study is shown in Figures 2 and 3, which give the pump-turbine's nominal diameter. The direct relationship between unit speed, unit torque, unit flow, and actual values in this model is as follows:

$$n_{11} = \omega_m \cdot D/\sqrt{h} \quad (1)$$

$$M_{11} = T_m \cdot D^3/\sqrt{h} \quad (2)$$

$$Q_{11} = Q \cdot D^2/\sqrt{h} \quad (3)$$

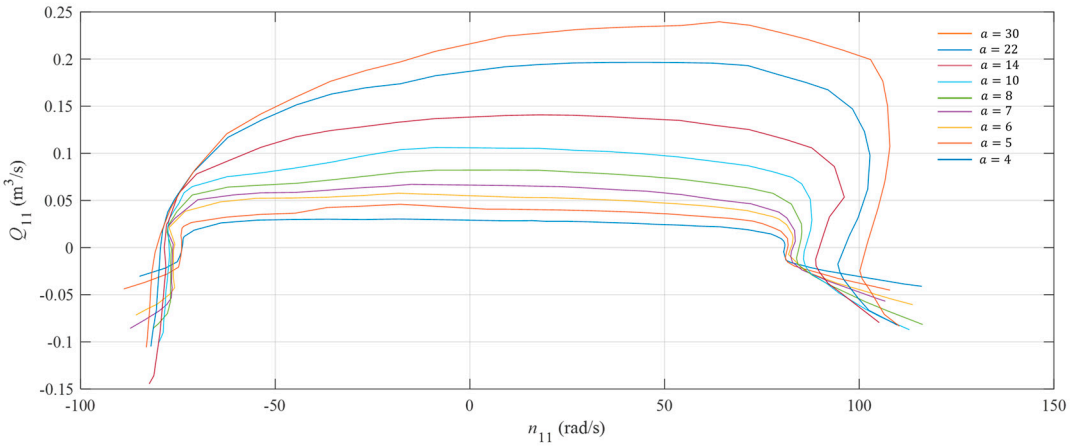

(**a**)

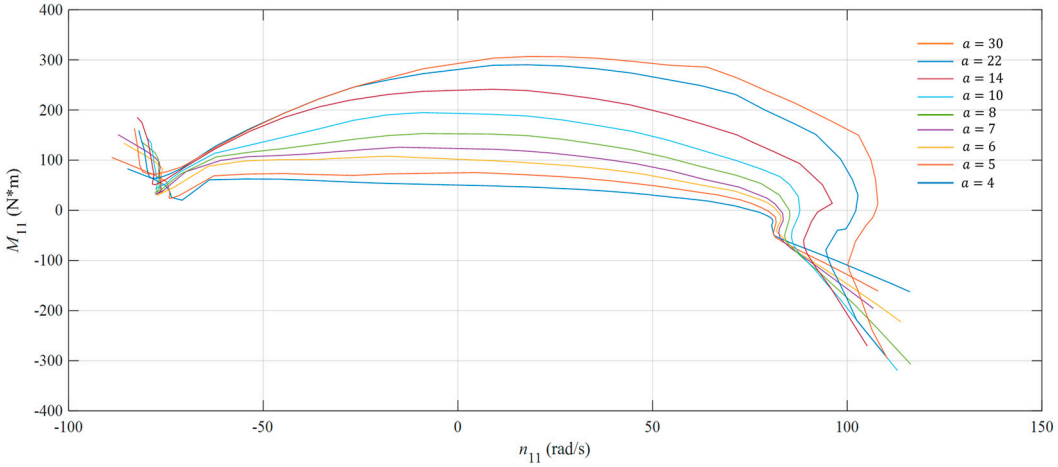

(**b**)

Figure 2. (**a**) Pump-turbine unit speed–unit flow rate total, characteristic curve. (**b**) Pump-turbine unit speed-unit torque entire, characteristic curve.

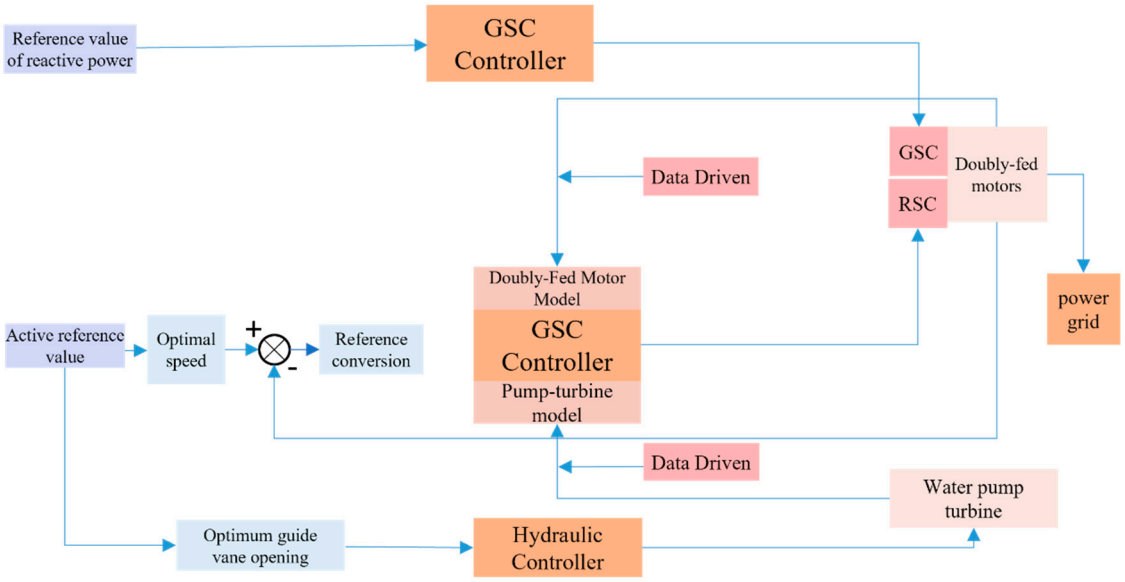

Figure 3. Control block diagram of variable-speed pumped storage unit.

2.2. Doubly-Fed Motor Model

Doubly-fed variable-speed pumped storage units are characterized by the use of AC-excited doubly-fed motors, which have a wide speed regulation range, can effectively reduce the impact of the grid voltage, reduce the electromagnetic interference of the system, and improve the stability and reliability of the system. The modeling principles in [15,18] are used.

2.2.1. Speed Relationship

The relationship between the stator synchronous speed and the rotor electrical speed of the doubly-fed motor is as follows, where ω_{sl} is defined as slip:

$$\omega_{sl} = \omega_s - \omega_m \tag{4}$$

The electrical speed of the rotor is related to the mechanical speed:

$$\omega_m = p \cdot \Omega_m \tag{5}$$

2.2.2. State-Space Representation of the Dynamic DFIM Power Model

The dynamic DFIM model is represented in a synchronized d-q reference system with a stator voltage orientation; the following equation is satisfied:

$$\begin{cases} v_{ds} = V_s \\ v_{qs} = 0 \end{cases}, \quad \begin{cases} \varphi_{ds} \approx 0 \\ \varphi_{qs} \approx -\dfrac{V_s}{\omega_s} \end{cases} \tag{6}$$

The electrical speed of the rotor is related to the mechanical speed:

$$\begin{cases} i_{ds} = \dfrac{1}{\sigma L_s L_r}(L_r \cdot \varphi_{ds} - L_m \cdot \varphi_{dr}) \\ i_{qs} = \dfrac{1}{\sigma L_s L_r}(L_r \cdot \varphi_{ds} - L_m \cdot \varphi_{dr}) \end{cases} \tag{7}$$

$$\begin{cases} v_{dr} = \dfrac{d}{dt}\varphi_{dr} - \omega_{sl} \cdot \varphi_{qr} \\ v_{qr} = \dfrac{d}{dt}\varphi_{qr} + \omega_{sl} \cdot \varphi_{dr} \end{cases} \tag{8}$$

The active and reactive power output of the doubly-fed motor can be expressed as follows:

$$\begin{cases} P_s = \dfrac{3}{2}(v_{ds} \cdot i_{ds} + v_{qs} \cdot i_{qs}) \\ Q_s = \dfrac{3}{2}(v_{qs} \cdot i_{ds} - v_{ds} \cdot i_{qs}) \end{cases} \tag{9}$$

Substituting Equations (6)–(8) into (9) can be simplified as follows:

$$\begin{cases} P_s = -\dfrac{3}{2} \cdot V_s \cdot \dfrac{L_m}{\sigma L_s L_r}\varphi_{dr} \\ Q_s = \dfrac{3}{2} \cdot V_s \cdot \dfrac{L_m}{\sigma L_s L_r} \cdot (L_r \cdot \dfrac{V_s}{w_s} + L_m \cdot \varphi_{qr}) \end{cases} \tag{10}$$

The dynamic equations of active and reactive power can be obtained by first-order derivation of the above equation as follows:

$$\begin{cases} \dfrac{d}{dt}P_s = -H_m V_s L_m \cdot \dfrac{d}{dt}\varphi_{dr} \\ \dfrac{d}{dt}Q_s = H_m V_s L_m \cdot \dfrac{d}{dt}\varphi_{qr} \end{cases} \tag{11}$$

where:

$$H_m = \frac{3}{2}\frac{1}{\sigma L_s L_r}$$

When combined with Equation (8), the state-space equations are obtained:

$$\frac{d}{dt}\begin{bmatrix} P_s \\ Q_s \end{bmatrix} = \begin{bmatrix} 0 & -\omega_{sl} \\ \omega_{sl} & 0 \end{bmatrix}\begin{bmatrix} P_s \\ Q_s \end{bmatrix} + \begin{bmatrix} -H_m V_s L_m & 0 \\ 0 & H_m V_s L_m \end{bmatrix}\begin{bmatrix} v_{dr} \\ v_{qr} \end{bmatrix} + \begin{bmatrix} \omega_{sl} H_m {V_s}^2 L_r/\omega_s \\ 0 \end{bmatrix} \quad (12)$$

The reference transformation is the process of converting the speed reference value to the stator active power reference value of the doubly-fed motor, as shown in the following equation:

$$Ps_{ref} = -\frac{3}{2} p \frac{L_m}{L_s} V_s \cdot k_{ex} \cdot (\omega_{mref} + \omega_{sref}) \quad (13)$$

2.2.3. Oscillation Equation Model

The swing equation of the doubly-fed motor, including the damping term, is as follows:

$$T_a \frac{d\Omega_m}{dt} = \frac{T_a}{p}\frac{d\omega_m}{dt} = T_m - T_{em} - D_t \Delta\omega_m \quad (14)$$

where T is the mechanical time constant.

2.3. Modeling the Water Diversion System

The pressure piping system can be modeled with an approximate elastic water hammer model with the following expression:

$$G(S) = \frac{-T_w s}{0.125 {T_r}^2 s^2 + f T_r s + 1} \quad (15)$$

where T_w is the water inertia time constant, T_r is the reflection time of water hammer pressure, and f is the head loss coefficient.

3. Data-Driven Model-Based Predictive Control Method under Power Generation Conditions

3.1. Control Strategy

In terms of control mode, the pump-turbine and double-fed motor have independent control systems, and achieving their cooperation is an important research direction in the development of the control strategy. There are three control strategy ideas: ① control the output power of the unit using the control system of the double-fed motor, and control the rotational speed using the control system of the pump-turbine by adjusting the opening degree of the guide vane; ② control the rotational speed using the control system of the double-fed motor, and control the power using the control system of the pump-turbine; ③ the combination of the first two ideas—power control. As we have decoupled the motor speed from the grid frequency, the system loses its inertia support ability, which significantly reduces the ability of the system to resist disturbance and regulate the active frequency, thus increasing the difficulty of system frequency regulation. The control strategy proposed in this paper utilizes rotational speed master control to maintain the flexibility of the DFIM speed adjustability and ensure a rapid response when short-term fluctuations in the grid frequency occur. This method can give full play to the advantages of pumped storage power plants in the new power system and enhance the stability and reliability of the system. Therefore, this paper adopts the ② control strategy to improve the power response speed of the unit. A schematic diagram of the control strategy is given in Figure 3.

3.2. Pump-Turbine Control System

The pump-turbine control system mainly consists of a hydraulic controller, as shown in Figure 4, and when compared with the traditional pumped storage units, the doubly-fed pumped storage units need an optimal guide vane opening generator.

The control block diagrams of hydraulic controllers under turbine and pump conditions are shown in Figures 5 and 6. The main difference between the hydraulic controllers under the two conditions is the control strategy for the guide vane opening. Under turbine conditions, this is mainly used to regulate the water flow into the turbine, and to control the rotational speed and output power of the unit. The opening of the guide vane has a direct impact on the efficiency and stability of the turbine. In the pump condition, the guide vane is used to control the water flow into the pump, to regulate the suction volume and pumping power. The opening of the guide vane affects the pump's working point and operating efficiency. Therefore, as shown in Figure 5, the hydraulic controller under turbine conditions uses the closed-loop control loop of the guide vane opening. As shown in Figure 6, the hydraulic controller under pump conditions directly uses an open-loop control of the guide vane opening.

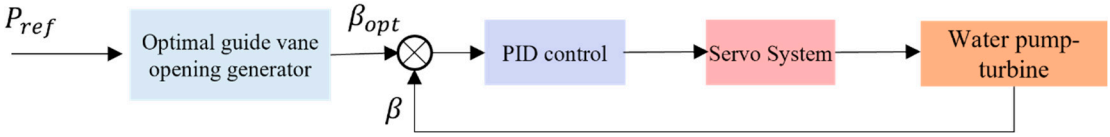

Figure 4. Hydraulic controller turbine operating condition control block diagram.

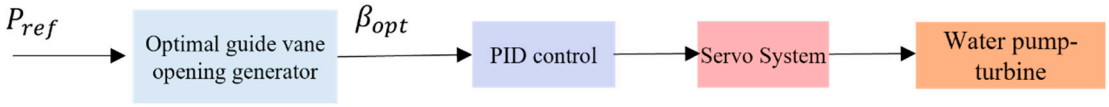

Figure 5. Hydraulic controller pump working condition control block diagram.

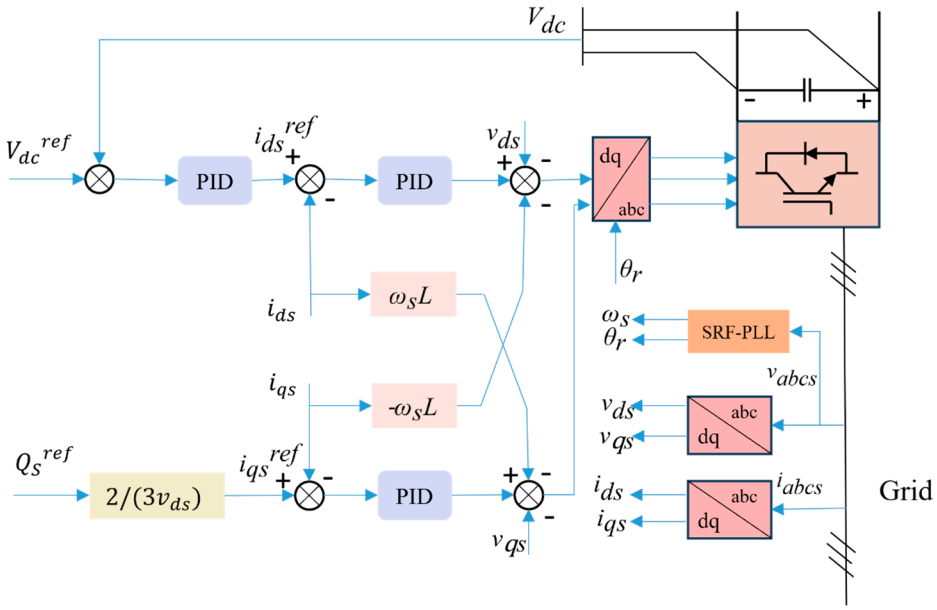

Figure 6. GSC controller control scheme.

3.3. Doubly-Fed Motor Control System

The doubly-fed motor control system realizes the control and operation of the doubly-fed motor through the cooperation of two controllers, GSC and RSC. The primary function of the GSC is to provide a constant DC bus voltage for the RSC, and it can also provide reactive power support for the power grid if needed. At the same time, the RSC

regulates the rotor current of the motor through the control circuit, to realize a high efficiency of motor operation and precise control. In this paper, vector control is used in the GSC, and we emphasize the potential to use a data-driven model predictive control technique to realize the RSC control. The two control approaches are described as follows:

3.3.1. Vector Control of GSC

The GSC regulates the DC bus voltage, shared with the RSC, while its AC side is connected to the grid. The GSC can receive or send active power according to the DFIG's operating mode. Therefore, the GSC is responsible for controlling the current between the GSC and the grid and regulating the DC bus voltage of the RSC. The GSC control structure is shown in Figure 7, where the grid angle θ_s and angular frequency ω_s are obtained by combining a phase-locked loop SRF-PLL with the measured three-phase grid voltage.

The control scheme uses two current control loops: one for the d-axis current i_{gd} control loop and the other for the q-axis current i_{gq} control loop. The control inputs use the reference values of DC bus voltage and grid reactive power, where the DC bus voltage satisfies Equation (16), and the current loop equations can be obtained from the DFIG model in the form of Equation (17).

$$C\frac{dv_{dc}}{dt} = i_{dc} - \frac{3}{2}\frac{V_s}{v_{dc}} \cdot i_{gd} \tag{16}$$

$$\begin{cases} v_{ds} = -L\dfrac{di_{ds}}{dt} - Ri_{qs} + \omega_s Li_{qs} + v_d \\ v_{qs} = -L\dfrac{di_{qs}}{dt} - Ri_{qs} - \omega_s Li_{ds} + v_q \end{cases} \tag{17}$$

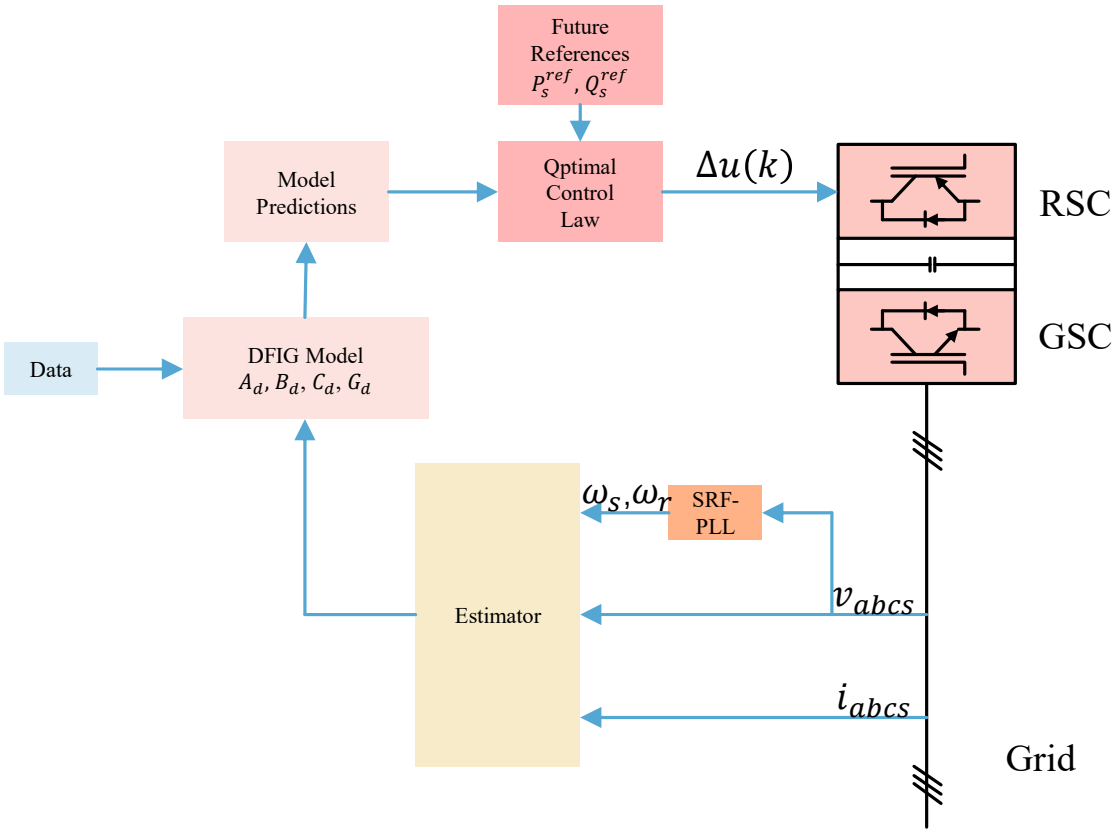

Figure 7. RSC model predictive controller control scheme.

3.3.2. Data-Driven RSC Model Predictive Controller

The optimal rotational speed ω_{opt} is obtained from the active power reference value P_{ref}, and its derivation process is based on the optimization-seeking idea of load optimization regulation theory [26] and combined with the BP neural network.

The state-space model of the doubly-fed motor shown in Equation (12) can be represented in the following form:

$$\begin{cases} \dfrac{d}{dt}\bar{x} = A\bar{x} + B\bar{u} + G\bar{o} \\ \bar{y} = C\bar{x} \end{cases} \tag{18}$$

By converting it into discrete form, it can be expressed in the form of Equation (19), and then the discrete model of the doubly-fed motor is shown in Equation (20).

$$\begin{cases} \bar{x}(k+1) = A_d\bar{x}(k) + B_d\bar{u}(k) + G_d\bar{o}(k) \\ \bar{y}(k+1) = C_d\bar{x}(k+1) \end{cases}$$
$$A_d = I + AT_s, B_d = BT_s, G_d = GT_s, C_d = C \tag{19}$$

$$\begin{bmatrix} P_s(k+1) \\ Q_s(k+1) \end{bmatrix} = \begin{bmatrix} 1 & -T_s\omega_{sl} \\ T_s\omega_{sl} & 1 \end{bmatrix} \cdot \begin{bmatrix} P_s(k) \\ Q_s(k) \end{bmatrix} + \begin{bmatrix} -T_sH_mV_sL_m & 0 \\ 0 & T_sH_mV_sL_m \end{bmatrix} \begin{bmatrix} v_{dr}(k) \\ v_{qr}(k) \end{bmatrix} + I \cdot \begin{bmatrix} T_s\omega_{sl}H_mV_s{}^2L_r/\omega_s \\ 0 \end{bmatrix} \tag{20}$$

A difference operation on Equation (19) yields the following:

$$\begin{cases} \Delta\bar{x}(k+1) = A_d\Delta\bar{x} + B_d\Delta\bar{u} + G_d\Delta\bar{o} \\ \Delta\bar{y}(k+1) = C_d\Delta\overline{x(k+1)} \end{cases} \tag{21}$$

Here, we assume that the control error is shown below, where *r(k)* is the control reference.

$$e(k) = \bar{y}(k) - r(k) \tag{22}$$

The differential form can be expressed as follows:

$$\Delta e(k+1) = e(k+1) - e(k) = \Delta\bar{y}(k+1) - \Delta r(k+1) \tag{23}$$

Transformations can be obtained:

$$\begin{aligned} e(k+1) &= e(k) + C_d\Delta\bar{y}(k+1) - \Delta r(k+1) \\ &= e(k) + C_dA_d\Delta\bar{x}(k) + C_dB_d\Delta\bar{u}(k) + C_dG_d\Delta\bar{o}(k) - \Delta r(k+1) \end{aligned} \tag{24}$$

We take the extended state variable as follows:

$$z(k) = [\Delta\bar{x}(k), e(k)]^T \tag{25}$$

Then, the state-space model can be written as Equation (26).

$$\begin{aligned} z(k+1) &= \begin{bmatrix} \Delta\bar{x}(k+1) \\ e(k+1) \end{bmatrix} \\ &= \begin{bmatrix} A_d & 0 \\ C_dA_d & 0 \end{bmatrix} \cdot \begin{bmatrix} \Delta\bar{x}(k) \\ e(k) \end{bmatrix} + \begin{bmatrix} B_d \\ C_DB_d \end{bmatrix} \cdot \Delta\bar{u}(k) + \begin{bmatrix} G_d \\ G_dB_d \end{bmatrix} \cdot \Delta\bar{o}(k) + \begin{bmatrix} 0 \\ -1 \end{bmatrix} \cdot \Delta r(k) \\ &= \tilde{A} \cdot z(k) + \tilde{B}\Delta\bar{u}(k) + \tilde{G}\Delta\bar{o}(k) + \tilde{C} \cdot \Delta r(k) \end{aligned} \tag{26}$$

Here, the level of control is chosen to be m. According to the model shown in Equation (21), the prediction of the future at moment k can be obtained as follows:

$$Z = S \cdot z(k) + F \cdot \Delta U + K \cdot \Delta O + T \cdot \Delta R \tag{27}$$

where:

$$Z = \begin{bmatrix} z(k+1) \\ z(k+2) \\ \vdots \\ \Delta r(k+P) \end{bmatrix}, \Delta U = \begin{bmatrix} \Delta \bar{u}(k) \\ \Delta \bar{u}(k+1) \\ \vdots \\ \Delta \bar{u}(k+M-1) \end{bmatrix}, \Delta O = \begin{bmatrix} \Delta \bar{o}(k+1) \\ \Delta \bar{o}(k+2) \\ \vdots \\ \Delta \bar{o}(k+P) \end{bmatrix},$$

$$\Delta R = \begin{bmatrix} \Delta \bar{r}(k+1) \\ \Delta \bar{r}(k+2) \\ \vdots \\ \Delta r(k+P) \end{bmatrix}, S = \begin{bmatrix} \tilde{A} \\ \tilde{A}^2 \\ \tilde{A}^3 \\ \vdots \\ \tilde{A}^P \end{bmatrix}$$

$$F = \begin{bmatrix} \tilde{B} & 0 & 0 & \dots & 0 \\ \tilde{A}\tilde{B} & \tilde{B} & 0 & \dots & 0 \\ \tilde{A}^2\tilde{B} & \tilde{A}\tilde{B} & \tilde{B} & \dots & 0 \\ \vdots & \vdots & \vdots & \ddots & \vdots \\ \tilde{A}^{P-1}\tilde{B} & \tilde{A}^{P-2}\tilde{B} & \tilde{A}^{P-3}\tilde{B} & \dots & \tilde{A}^{P-M}\tilde{B} \end{bmatrix}$$

$$K = \begin{bmatrix} \tilde{G} & 0 & 0 & \dots & 0 \\ \tilde{A}\tilde{G} & \tilde{G} & 0 & \dots & 0 \\ \tilde{A}^2\tilde{G} & \tilde{A}\tilde{G} & \tilde{G} & \dots & 0 \\ \vdots & \vdots & \vdots & \ddots & \vdots \\ \tilde{A}^{P-1}\tilde{G} & \tilde{A}^{P-2}\tilde{G} & \tilde{A}^{P-3}\tilde{G} & \dots & \tilde{A}^{P-M}\tilde{G} \end{bmatrix},$$

$$T = \begin{bmatrix} \tilde{C} & 0 & 0 & \dots & 0 \\ \tilde{A}\tilde{C} & \tilde{C} & 0 & \dots & 0 \\ \tilde{A}^2\tilde{C} & \tilde{A}\tilde{C} & \tilde{C} & \dots & 0 \\ \vdots & \vdots & \vdots & \ddots & \vdots \\ \tilde{A}^{P-1}\tilde{C} & \tilde{A}^{P-2}\tilde{C} & \tilde{A}^{P-3}\tilde{C} & \dots & \tilde{A}^{P-M}\tilde{C} \end{bmatrix}$$

The control law is obtained from the minimum of the following cost function, in which the model is linearized, and the minimum can be determined algebraically. Because SFKTs depend on the estimated state, they must be updated in each control cycle.

$$J = min(Z^T \cdot Q \cdot Z + \Delta U^T \cdot L \cdot \Delta U) \tag{28}$$

Substituting Equation (22) into Equation (23) yields a quadratic cost function dependent on the control increment with the following optimal analytic solution:

$$\Delta U = -(F^T \cdot Q \cdot F + L)^{-1} F^T Q \cdot [S \cdot z(k) + K \cdot \bar{o}(k) + T \cdot r(k)] \tag{29}$$

4. Simulation Results

A simulation experiment of the control strategy was carried out using MATLAB/Simulink with a simulation step size of 5×10^{-5} s. The background of the experiment was a microgrid consisting of photovoltaics, wind power, a variable-speed pumping unit, a diesel generator set, and auxiliary pumping pumps, where the power assumed by each device was as shown in Figure 8a. The doubly-fed motor control system controlled the output power of the unit. The pump-turbine control system controlled the speed by adjusting the opening of the guide vane. In the steady-state operation of the variable-speed pumping and storage unit, the opening of the guide vane of the water pump-turbine was optimized and calculated. The results are shown in Figure 8b, which gives the distribution of the optimal opening of the guide vane. These data were directly used as the control signals to implement the adjustment of the guide vane through the sophisticated servo system. In conjunction with the adjustment of the guide vane opening, the optimal selection of the rotational speed was also carefully calculated, and the results are shown in Figure 8c, which guided the control strategy of the power converter and ensured the optimization of the output power of the pumped storage system.

In order to test the dynamic response of the proposed model predictive control strategy for the electrical quantity when the output power of variable-speed pumped storage unit changed, we selected the two cases of a rise and fall in output active power under a

power generation condition and pumping condition, respectively, as shown in Figure 9a–d, of which (a) is the case of a rise in output power under the power generation condition, where the power rises from 151.93 MW to 161.50 MW; (b) is the case of a power decrease in the generation condition, with the power decreasing from 168.38 MW to 129.76 MW; (c) is the case of a power increase in the pumping condition, with the power increasing from 115.38 MW to 120 MW; and (d) is the case of a power decrease in the pumping condition, with the power decreasing from 194.21 MW to 140.63 MW.

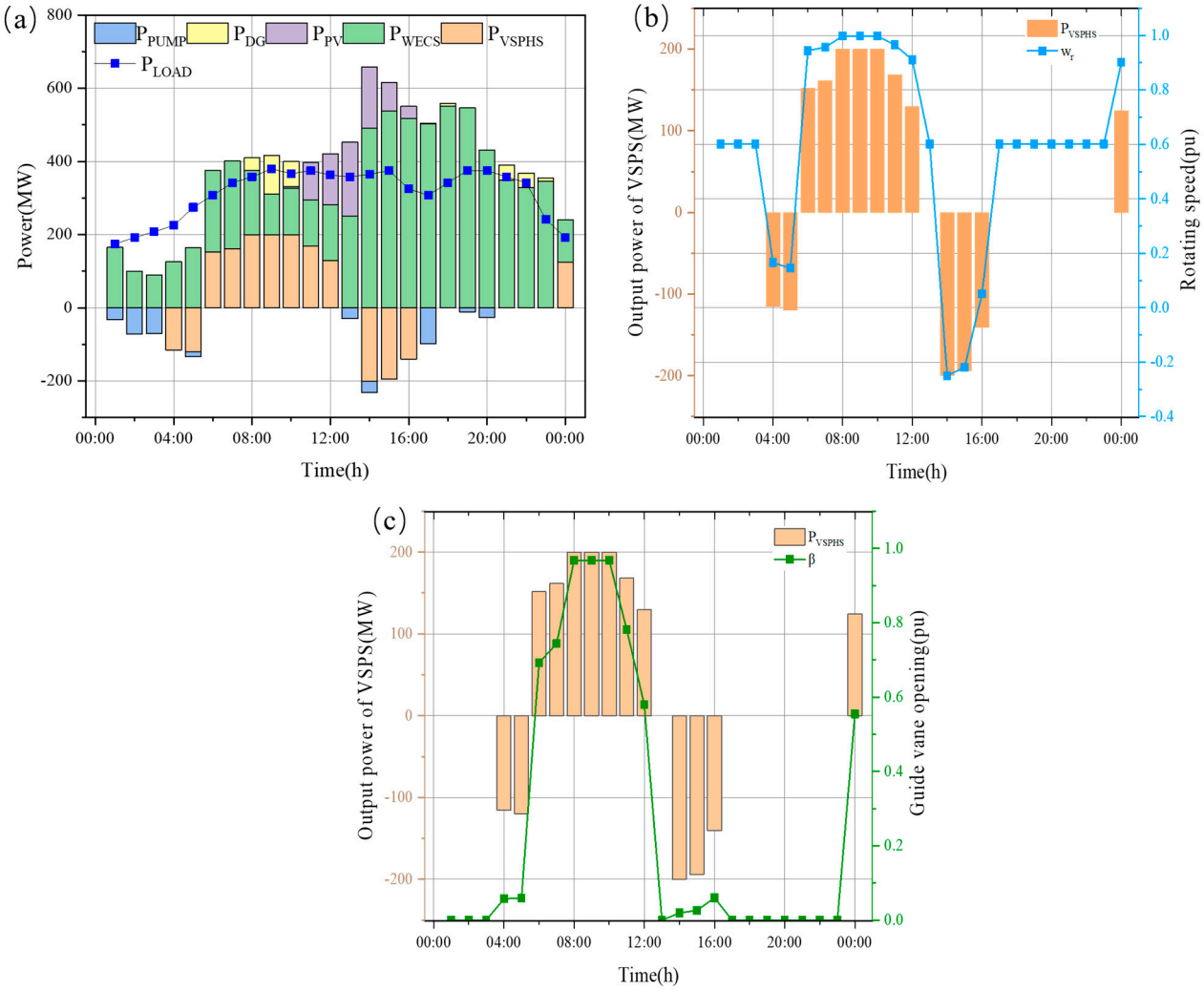

Figure 8. (**a**) Power distribution diagram; (**b**) optimization results of guide vane opening; (**c**) speed optimization results.

4.1. Simulation Results of Output Active Power

The simulation results of the output active power for four working conditions are shown in Figure 10, where P_ref is the reference value of output active power, P_PID(opt) represents the control response after optimization of PID parameters, P_PID(Nopt) represents the control response with unoptimized PID parameters, and P_MPC is the response of MPC in this paper.

For the steady-state error, the PID controller with unoptimized parameters can eventually reach a steady state, but with more oscillations. Both the optimized PID controller and the MPC controller can effectively eliminate the steady-state error and closely track the reference signal.

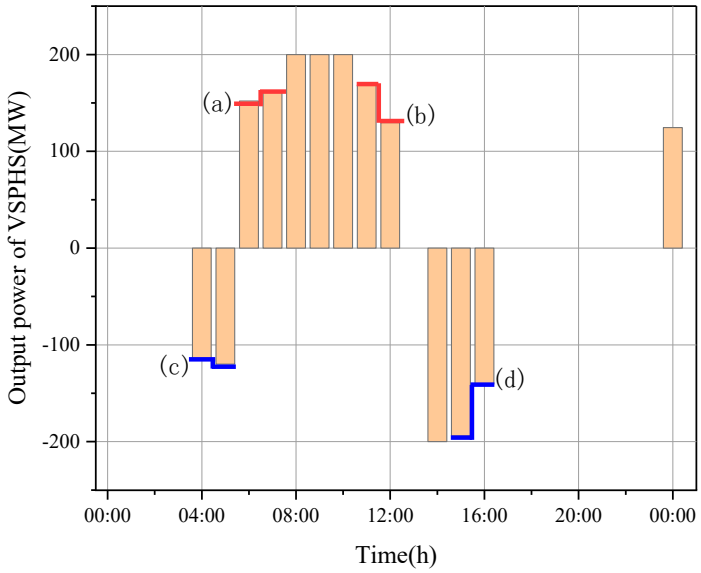

Figure 9. (**a**) Power increases under power generation conditions. (**b**) The power output under power generation conditions decreases. (**c**) The power of the pumping condition increases. (**d**) The power of the pumping condition decreases.

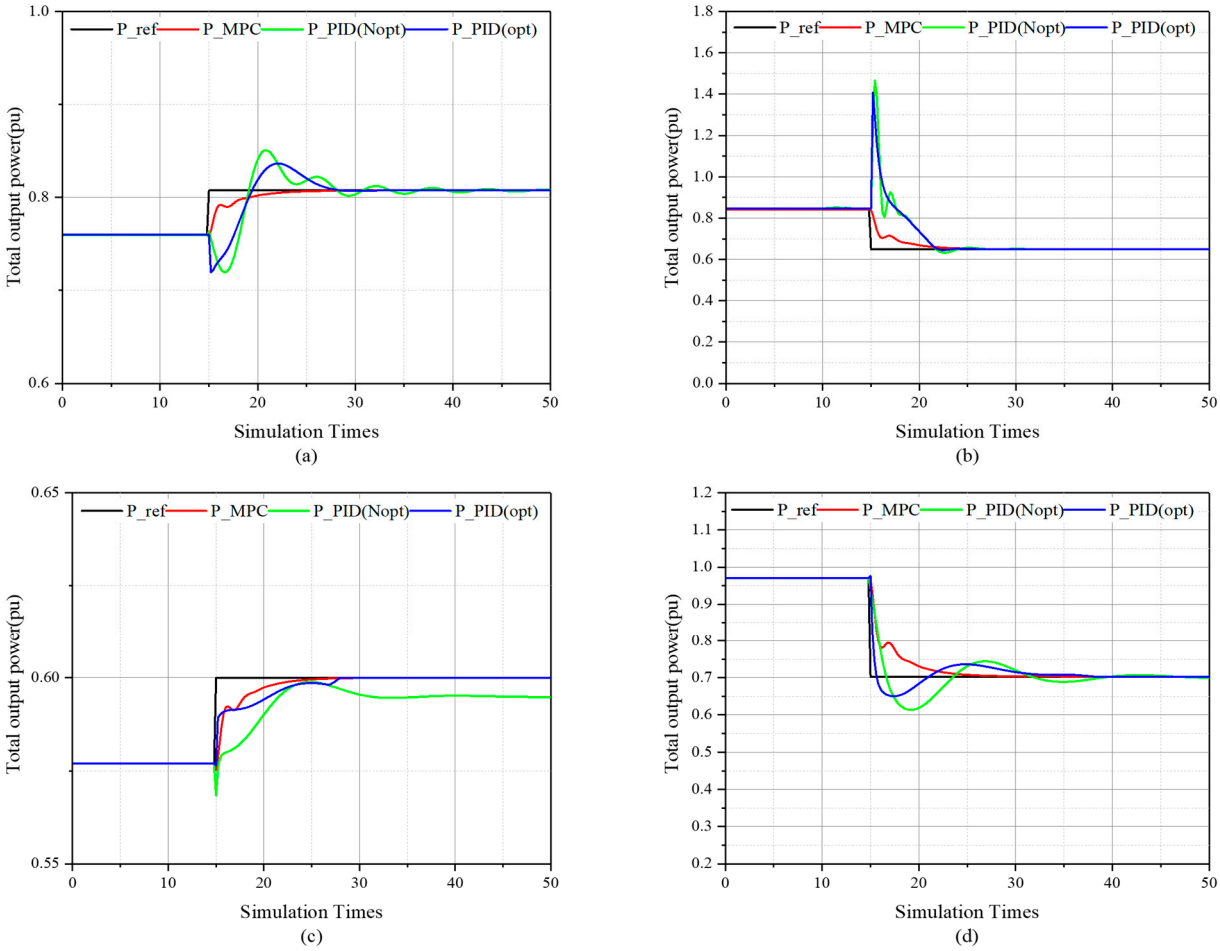

Figure 10. Simulation results of the active power output. (**a**) Results of the active power output when power increases under power generation conditions; (**b**) Results of the active power output when the power output under power generation conditions decreases; (**c**) Results of the active power output when the power of the pumping condition increases; (**d**) Results of the active power output when the power of the pumping condition decreases.

In terms of transient response, the unoptimized PID controller shows a delayed response with significant overshooting and oscillations, indicating poor control performance. The optimized PID controller shows a fast transient response with minimal overshooting and a better regulation performance. In contrast, the MPC controller has better stability and less overshooting, which is suitable for systems with higher stability requirements, but its response speed is slightly slower.

It can be seen that in the control process of variable-speed pumped storage units, the use of PID controllers requires the optimization of parameters, and the parameters, if not selected appropriately, will lead to larger overshoots and oscillations, indicating a poorer damping effect and control quality. In contrast, the MPC controller used in this paper can have a more minor overshoot and smoother response without the parameter optimization process.

In addition, due to the working principle based on global optimization and prediction, the MPC can consider and correct the control strategy in advance by predicting the future system response and performing rolling optimization in each control cycle, avoiding the type of tuning of PID controllers that relies solely on the current error, and thus reducing the magnitude of the overshoot.

4.2. Simulation Results of Variable-Speed Pumped Storage Units for Each Variable

4.2.1. Control Variables

The control variable simulation results of the variable-speed pumped storage unit are shown in Figure 11, including three control variables: the rotor speed w_r of the doubly-fed motor, the rotor q-axis voltage v_{qr}, and the guide vane opening β.

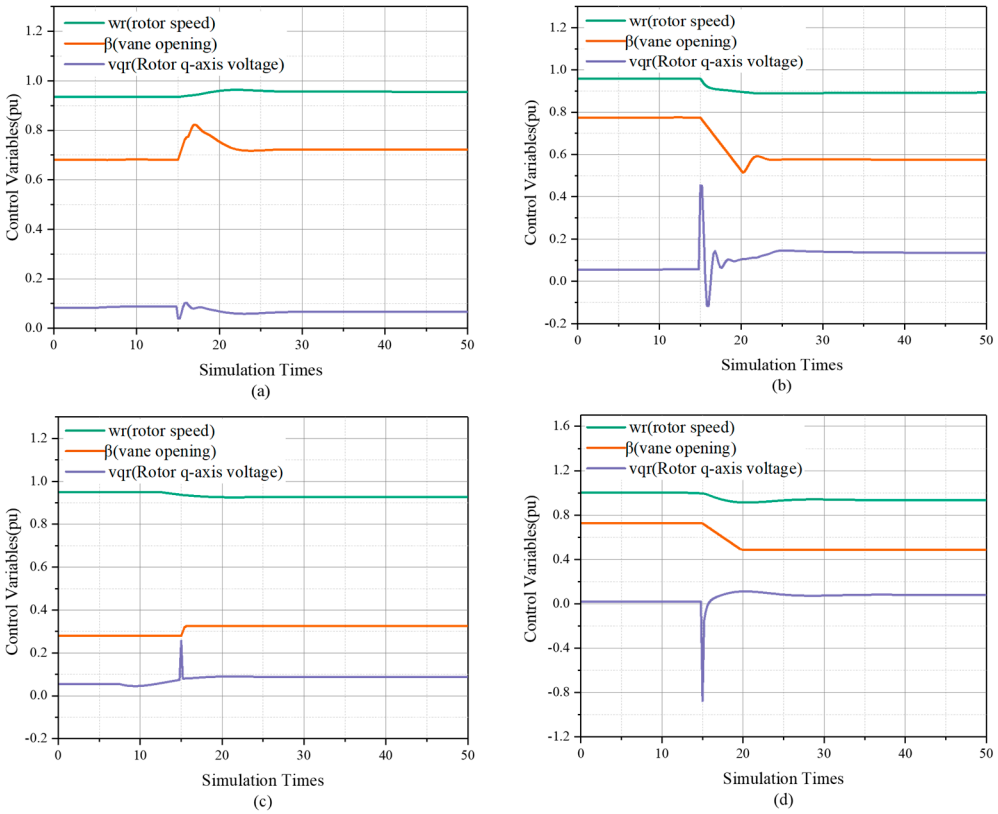

Figure 11. Simulation results for various variables of a variable-speed pumped storage unit. (**a**) Simulation results for various variables of a variable-speed pumped storage unit when power increases under power generation conditions. (**b**) Simulation results for various variables of a variable-speed pumped storage unit when the power output under power generation conditions decreases. (**c**) Simulation results for various variables of a variable-speed pumped storage unit when the power of the pumping condition increases. (**d**) Simulation results for various variables of a variable-speed pumped storage unit when the power of the pumping condition decreases.

As can be seen from this figure, the MPC controller is effective in maintaining the stability of the rotor speed, quickly adjusting, and restoring the speed to the target value when perturbed. The stability of the rotor speed is critical to the system's overall performance, and the MPC ensures it by predicting and regulating the rotor speed. At the same time, the MPC controller ensures that the guide vane opening varies within reasonable limits, thus avoiding over-or under-regulation. The most direct control variable for the MPC controller is the rotor q-axis voltage. The controller ensures that the voltage fluctuation is minimized during the system's operation through accurate voltage regulation, avoiding adverse effects on the rotor speed and the system's performance. The voltage's stability further reflects the MPC's superior performance under multivariable control.

4.2.2. Observed Variables

The observed variables include head h, flow q, and mechanical torque PT for the hydraulic system; and stator q-axis current i_{qs} and rotor q-axis current i_{qi} for the electrical system. The simulation results of the control process are shown in Figure 12.

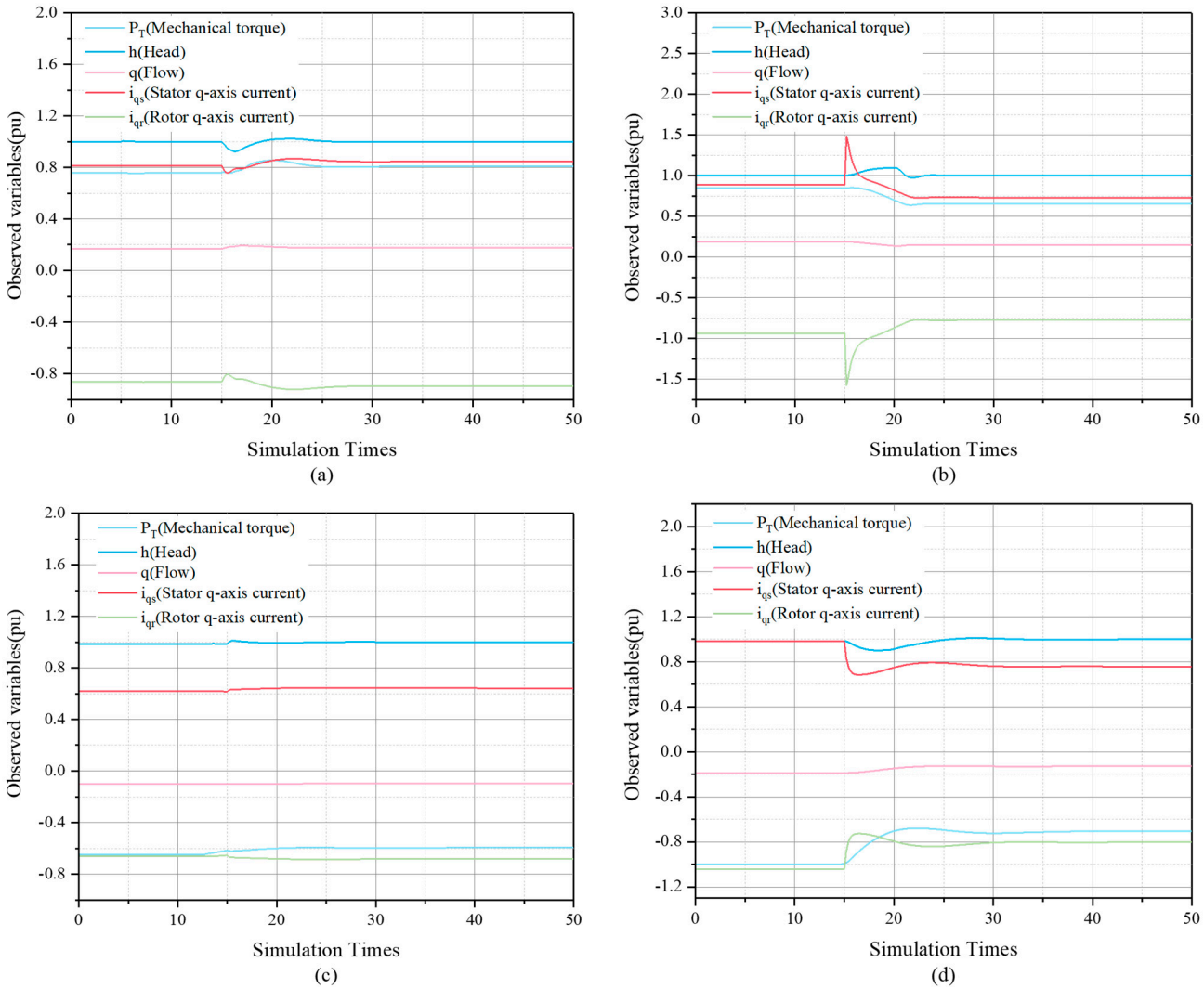

Figure 12. Simulation results of observed variables. (**a**) Simulation results of observed variables when power increases under power generation conditions. (**b**) Simulation results of observed variables when the power output under power generation conditions decreases. (**c**) Simulation results of observed variables when the power of the pumping condition increases. (**d**) Simulation results of observed variables when the power of the pumping condition decreases.

When observing the simulation results of the hydraulic and electrical variables, it can be seen that the MPC put forward in this paper realizes the multivariable optimal control of the complex system. The MPC maintains the system's stability and responsiveness under perturbation conditions and effectively manages the system's performance in a multivariable and multicentric environment. This control strategy is particularly suitable for complex electromechanical systems such as variable-speed pumped storage units, which can achieve efficient system operation while maintaining a steady-state performance.

However, while the MPC (model predictive control) demonstrates a powerful control performance and flexibility, its application also faces some limitations, and precautions should be taken. First, the computational complexity of MPC is high, which may affect its real-time performance, especially when the system is large, or the model is complex. Second, the performance of MPC is highly dependent on the accuracy of the system model, and model errors may lead to control decision errors. In addition, complex constraint processing and sensitivity to interference and model uncertainty are also challenges of the MPC. Third, when compared with traditional PID controllers, the implementation and maintenance of MPC are more complicated and require professional knowledge and skills, especially in parameter adjustment and initial value selection. To summarize these considerations, when proposing the application of MPC, it is necessary to weigh the tradeoff between its high performance and implementation complexity, as well as consider whether the provisions are in place to ensure model accuracy and sufficient computing power, and to reasonably handle constraints and uncertainties.

4.3. Comprehensive Performance Evaluation

In order to effectively compare the performance of the MPC strategy proposed in this paper with that of PID control, a Comprehensive Performance Index (CPI) was designed. The CPI combines the system's steady-state error, overshooting, tuning time, control energy, and robustness under different operating conditions to provide a comprehensive quantitative score for a control system. The CPI is calculated as follows, where the smaller the CPI value obtained, the better the combined performance of the system in all the performance indicators, and where the variable y is the total output power of the variable-speed pumped storage unit:

$$\mathrm{CPI} = w_1 \cdot \mathrm{SE} + w_2 \cdot \mathrm{OS} + w_3 \cdot \mathrm{ST} + w_4 \cdot \mathrm{CE} + w_5 \cdot (1 - \mathrm{RI})$$

Among the components here are the following:

① Steady-state error (SE), calculated by the difference between the output value and the set point after the system reaches a steady state:

$$\mathrm{SE} = |y_{\mathrm{ss}} - y_{\mathrm{ref}}|$$

② Overshoot (OS), the maximum percentage by which the output value exceeds the steady-state value during the system response:

$$\mathrm{OS} = \frac{\mathrm{yref}_{max}}{y_{\mathrm{ref}}\%}$$

③ Tuning time (ST), the time at which the system output first enters the specified error band, after which it remains there.

④ Control energy (CE), the total energy consumption when using the control input signal:

$$\mathrm{CE} = \int_0^T u(t)^2 dt$$

⑤ Robustness (RI), the ability of the control system to adapt to perturbations and changing conditions under different operating conditions, calculated using the active power output in the four operating conditions described above:

$$\mathrm{RI} = 1 - \frac{\sum_{i=1}^{N} \left(\mathrm{Mean}_{\Delta y_i} + \mathrm{SD}_{\Delta y_i}\right)}{N \cdot y_{\text{avg ref}}}$$

where:

N is the number of working conditions, taken as 4;

$Mean_{\Delta y_i}$ is the average absolute deviation between the system output and the reference value for the i-th working condition;

$\mathrm{SD}_{\Delta y_i}$ is the standard deviation of the output for the i-th working condition;

$y_{\text{avg ref}}$ is the average of the reference values for all working conditions.

Weights are set to $w_1 = 0.1, w_2 = 0.2, w_3 = 0.2, w_4 = 0.2$, and $w_5 = 0.3$. The weight selection process is as follows: all five weights are initially set to 0.2. Since both MPC and optimized PID must ensure the stable operation of the unit, the impact of stability (SE) is reduced to 0.1. The control method can lead the variable-speed pumped storage unit to be applicable under various working conditions, which is desirable, so the robustness weight (RI) is expanded to 0.3.

According to the above equations, the CPI values of MPC and PID control for a doubly-fed variable-speed pumped storage unit were calculated to be 0.083 and 0.126, respectively, and the distribution of each index is shown in Figure 13.

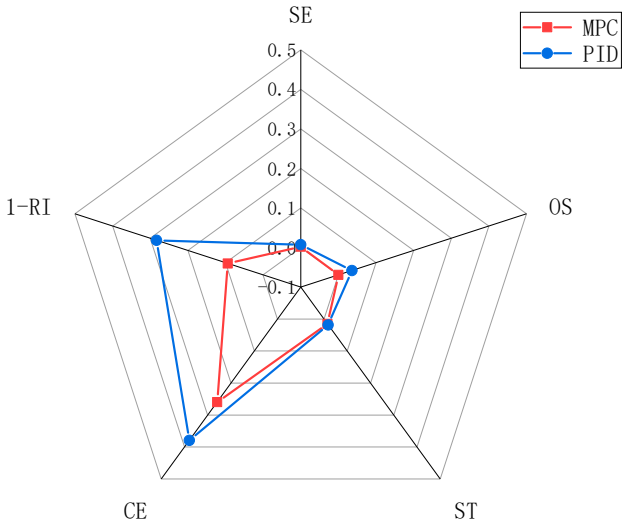

Figure 13. Schematic diagram of the distribution of various indicators.

Through experiments and simulations, we discerned that the MPC can better optimize the CPI metrics in complex multivariable systems, exhibiting a higher control accuracy and faster system response speed. This is because the MPC combines model prediction and optimization algorithms to predict future behaviors and optimize control signals at multiple time steps within each control cycle, thus handling system dynamics and complex constraints more efficiently. By explicitly handling input and output constraints, the MPC excels in multi-input and multi-output systems and optimizes the overall performance metrics for a better steady-state error, overshoot, tuning time, and control energy. In addition, the MPC demonstrates a better robustness in dealing with uncertainties and external perturbations. The robustness index (RI) of the MPC improved by 0.2 compared to the optimized PID control, which means there will be an improved control performance 20% of the time compared to the optimized PID control method when the operating conditions are frequently switched. This marks an effective improvement over the control robustness of variable-speed pumped storage units.

The introduction of data-driven technology further enhances the performance of MPC, which can better adapt to changes in system dynamics and the external

environment by accurately modeling the system of variable-speed pumped storage units. This dynamic adjustment capability allows MPC to exhibit greater flexibility and accuracy in complex or nonlinear systems, especially in rapidly changing or difficult-to-model scenarios.

5. Conclusions

This study has explored the application of a data-driven model predictive control (MPC) method in a doubly-fed variable-speed pumped storage unit and verified its effectiveness and superiority under complex working conditions through simulation. When compared with the traditional PID control method, the MPC algorithm significantly improves the control accuracy and response speed by predicting the future behavior of the system and optimizing the control input sequence in real time within each control cycle. The working principle of the MPC is based on the prediction and real-time optimization of the system model. It uses rolling optimization to minimize the tracking error and control cost within each control cycle, implements only the first control input in the optimal control sequence, and continuously adjusts the control strategy through a real-time feedback mechanism. This method effectively copes with the nonlinearity, time-varying characteristics, and multivariable coupling of the system and also realizes the dynamic optimization control of the system.

In the specific implementation process, we adopted a data-driven approach to build a prediction model of the system based on historical operation data, which was used to train the model parameters, improving the model's accuracy and robustness. Meanwhile, the control algorithm calculates the optimal control inputs in real time during each control cycle by solving an online optimization problem, enabling the system to respond quickly to external disturbances and load changes. In order to improve the computational efficiency and real-time performance of the algorithm, we also appropriately simplified and approximated the optimization problem.

In this study, simulation experiments were carried out on a variable-speed pumped storage unit model, and MPC exhibited a faster response speed and greater stability than the traditional PID control. During both power rise and fall, an MPC can quickly track the reference value, avoiding major overshooting and oscillation phenomena, realizing fast boosting, and showing a good dynamic response capability. Under power generation and pumping conditions, an MPC also performs well, avoiding the common oscillation and overshooting phenomena in a PID control, and ensuring a smooth response and high stability of the system in power change.

In addition, in the control of the rotational speed and guide vane opening, the MPC strategy ensures a smooth change in rotational speed and realizes the stable operation of the system by appropriately adjusting the guide vane opening in the regulation of electrical variables, particularly when the load changes, the transient response and stability of the rotor voltage are excellent. The calculation of the scores on the comprehensive evaluation indexes compiled in this study showed that the MPC strategy can improve the dynamic response speed of the system, reduce overshooting and oscillations, and maintain the system stability and robustness better than PID control in a complex multivariable system such as a variable-speed pumped storage unit.

This study has also shown that the data-driven MPC strategy has broad application prospects in doubly-fed variable-speed pumped storage units. By combining actual operating data with model predictive control, we achieved the accurate modeling and dynamic optimization control of complex systems, effectively dealing with the nonlinearity, multivariable coupling, and complex constraint problems of the system. Future research will further optimize the control algorithm to improve the response speed and stability of the system, and research will verify its efficacy in actual engineering to promote the application and promotion of this technology. This innovative control method is expected to significantly improve the operating efficiency and reliability of pumped storage units, and in doing so, provide a solid guarantee of the efficient use of new energy.

Author Contributions: Conceptualization, Q.C.; methodology, Q.C.; software, P.Z.; validation, P.Z., Q.C. and C.G.; formal analysis, P.Z.; investigation, C.G., Q.C. and P.Z.; resources, H.N.; data curation, C.G., Q.C. and L.W.; writing—original draft preparation, P.Z.; writing—review and editing, P.Z., Q.C. and C.G.; visualization, C.G. and L.W.; supervision, P.Z. and Q.C.; project administration, C.G. and Q.C.; funding acquisition, Q.C. and L.W. All authors have read and agreed to the published version of the manuscript.

Funding: This research was funded by Shaanxi Provincial Education Department (NO. 23JE012).

Data Availability Statement: All relevant data are within the paper.

Acknowledgments: The authors would like to sincerely thank the editor and anonymous reviewers. for their valuable comments and suggestions to improve the quality of the article.

Conflicts of Interest: Author Qingsen Cai was employed by the Northwest Engineering Corporation Limited. The remaining authors declare that the research was conducted in the absence of any commercial or financial relationships that could be construed as a potential conflict of interest.

References

1. IRENA—International Renewable Energy Agency. *Renewable Capacity Statistics 2023*; IRENA: New York, NY, USA, 2023.
2. Elliott, D. A balancing act for renewables. *Nat. Energy* **2016**, *1*, 15003. https://doi.org/10.1038/nenergy.2015.3.
3. Pérez-Díaz, J.I.; Chazarra, M.; García-González, J.; Cavazzini, G.; Stoppato, A. Trends and challenges in the operation of pumped-storage hydropower plants. *Renew. Sustain. Energy Rev.* **2015**, *44*, 767–784. https://doi.org/10.1016/j.rser.2015.01.029.
4. Liu, L.; Sun, Q.; Li, H.; Yin, H.; Ren, X.; Wennersten, R. Evaluating the benefits of Integrating Floating Photovoltaic and Pumped Storage Power System. *Energy Convers. Manag.* **2019**, *194*, 173–185. https://doi.org/10.1016/j.enconman.2019.04.071.
5. Yang, W.; Yang, J. Advantage of variable-speed pumped storage plants for mitigating wind power variations: Integrated modelling and performance assessment. *Appl. Energy* **2019**, *237*, 720–732. https://doi.org/10.1016/j.apenergy.2018.12.090.
6. Koritarov, V.; Veselka, T.D.; Gasper, J.; Bethke, B.M.; Botterud, A.; Wang, J.; Mahalik, M.; Zhou, Z. *Modeling and Analysis of Value of Advanced Pumped Storage Hydropower in the United States*; Argonne National Lab.: Argonne, IL, USA, 2014.
7. Vasudevan, K.R.; Ramachandaramurthy, V.K.; Venugopal, G.; Ekanayake, J.; Tiong, S. Variable speed pumped hydro storage: A review of converters, controls and energy management strategies. *Renew. Sustain. Energy Rev.* **2021**, *135*, 110156. https://doi.org/10.1016/j.rser.2020.110156.
8. Fang, H.; Chen, L.; Shen, Z. Application of an improved PSO algorithm to optimal tuning of PID gains for water turbine governor. *Energy Convers. Manag.* **2011**, *52*, 1763–1770. https://doi.org/10.1016/j.enconman.2010.11.005.
9. Gao, C.; Yu, X.; Nan, H.; Men, C.; Zhao, P.; Cai, Q.; Fu, J. Stability and dynamic analysis of doubly-fed variable speed pump turbine governing system based on Hopf bifurcation theory. *Renew. Energy* **2021**, *175*, 568–579. https://doi.org/10.1016/j.renene.2021.05.015.
10. Hušek, P. PID controller design for hydraulic turbine based on sensitivity margin specifications. *Int. J. Electr. Power Energy Syst.* **2014**, *55*, 460–466. https://doi.org/10.1016/j.ijepes.2013.09.029.
11. Xu, Y.; Zhou, J.; Xue, X.; Fu, W.; Zhu, W.; Li, C. An adaptively fast fuzzy fractional order PID control for pumped storage hydro unit using improved gravitational search algorithm. *Energy Convers. Manag.* **2016**, *111*, 67–78. https://doi.org/10.1016/j.enconman.2015.12.049.
12. Huang, S.; Zhou, B.; Bu, S.; Li, C.; Zhang, C.; Wang, H.; Wang, T. Robust fixed-time sliding mode control for fractional-order nonlinear hydro-turbine governing system. *Renew. Energy* **2019**, *139*, 447–458. https://doi.org/10.1016/j.renene.2019.02.095.
13. Zhang, R.; Chen, D.; Ma, X. Nonlinear Predictive Control of a Hydropower System Model. *Entropy* **2015**, *17*, 6129–6149. https://doi.org/10.3390/e17096129.
14. Liang, L.; Hou, Y.; Hill, D.J. GPU-Based Enumeration Model Predictive Control of Pumped Storage to Enhance Operational Flexibility. *IEEE Trans. Smart Grid* **2019**, *10*, 5223–5233. https://doi.org/10.1109/tsg.2018.2879226.
15. Sguarezi, A.J. and E. Ruppert, Model-Based Predictive Control Applied to the Doubly-Fed Induction Generator Direct Power Control. *IEEE Trans. Sustain. Energy* **2012**, *3*, 398–406.
16. Errouissi, R.; Al-Durra, A.; Muyeen, S.M.; Leng, S.; Blaabjerg, F. Offset-Free Direct Power Control of DFIG Under Continuous-Time Model Predictive Control. *IEEE Trans. Power Electron.* **2017**, *32*, 2265–2277. https://doi.org/10.1109/tpel.2016.2557964.
17. Zhou, C.; Wang, Z.; Xin, H.; Ju, P. A P-Q Coordination Based Model Predictive Control for DFIG High-Voltage Ride Through. *IEEE Trans. Energy Convers.* **2022**, *37*, 254–263. https://doi.org/10.1109/tec.2021.3088464.
18. Hui, L.I.; Li, H.A.N.; Bei, H.E. Simulation for Strategy of Maximal Wind Energy Capture and Conversion of Doubly Fed Induction Generators. *J. Syst. Simul.* **2007**, *19*, 3591–3594.
19. Kazemi, M.V.; Sadati, S.J.; Gholamian, S.A. Adaptive frequency control support of a DFIG based on second-order derivative controller using data-driven method. *Int. Trans. Electr. Energy Syst.* **2020**, *30*, 12424. https://doi.org/10.1002/2050-7038.12424.
20. Yin, X.; Zhao, X. Data driven learning model predictive control of offshore wind farms. *Int. J. Electr. Power Energy Syst.* **2021**, *127*, 106639. https://doi.org/10.1016/j.ijepes.2020.106639.

21. Carlet, P.G.; Favato, A.; Bolognani, S.; Dorfler, F. Data-Driven Continuous-Set Predictive Current Control for Synchronous Motor Drives. *IEEE Trans. Power Electron.* **2022**, *37*, 6637–6646. https://doi.org/10.1109/tpel.2022.3142244.
22. Carlet, P.G.; Favato, A.; Torchio, R.; Toso, F.; Bolognani, S.; Dorfler, F. Real-Time Feasibility of Data-Driven Predictive Control for Synchronous Motor Drives. *IEEE Trans. Power Electron.* **2023**, *38*, 1672–1682. https://doi.org/10.1109/tpel.2022.3214760.
23. Cai, Q.; Luo, X.; Gao, C.; Guo, P.; Sun, S.; Yan, S.; Zhao, P. A Machine Learning-Based Model Predictive Control Method for Pumped Storage Systems. *Front. Energy Res.* **2021**, *9*. https://doi.org/10.3389/fenrg.2021.757507.
24. Feng, C.; Li, C.; Chang, L.; Mai, Z.; Wu, C. Nonlinear Model Predictive Control for Pumped Storage Plants Based on Online Sequential Extreme Learning Machine with Forgetting Factor. *Complexity* **2021**, *2021*, 5692621. https://doi.org/10.1155/2021/5692621.
25. Zheng, X.B.; Tong, H.Z. Improvement of Suter transformation for the full characteristic curve of water pump turbine.Journal of Irrigation and Drainage Machinery Engineering. *J. Irrig. Drain. Mach. Eng.* **2013**, *31*, 1061–1064+1104.
26. Reigstad, T.I.; Uhlen, K. Optimized Control of Variable Speed Hydropower for Provision of Fast Frequency Reserves. *Electr. Power Syst. Res.* **2020**, *189*, 106668. https://doi.org/10.1016/j.epsr.2020.106668.

Disclaimer/Publisher's Note: The statements, opinions and data contained in all publications are solely those of the individual author(s) and contributor(s) and not of MDPI and/or the editor(s). MDPI and/or the editor(s) disclaim responsibility for any injury to people or property resulting from any ideas, methods, instructions or products referred to in the content.